J. Electron Spectrosc., accepted

Optical potential and escape depth for electron scattering at very low energies

Claus-Henning Solterbeck[a], Oliver Tiedje[a], Thomas Strasser[a], Sven Brodersen[a], Anke Bödicker[a], Wolfgang Schattke[a,*], Igor Bartoš[b]

(a) Institut für Theoretische Physik, Universität Kiel, Leibnizstraße 15, D-24118 Kiel, Germany

(b) Institute of Physics, Academy of Sciences of the Czech Republic, Cukrovarnická 10, 16253 Praha 6, Czech Republic

Electron spectroscopy at low kinetic energies, e.g. valence band photoemission with vacuum ultraviolet light, is sensitive to the fine structure of the electron damping, i.e. to the magnitude and energy dependence of the optical potential. The basis of this quantity is usually given by a semiquantitative analytical derivation together with empirical findings from the escape depth. Only recently the optical potential has been determined ab-initio via calculating the self-energy. Here, this approach is used to calculate the self-energy and from this the wavefunctions in the conduction band regime with scattering boundary conditions for the surface system. For the former, the GW approximation is applied. For the latter, algebraic solvers in the Laue representation have been used to solve the Schrödinger equation for arbitrary potentials. The wavefunction is investigated to extract physical quantities, like the angle and energy dependent escape depth, which are significant in discussing electron scattering.

The self-energy ($\mathbf{\Sigma}$) is the central quantity for characterizing many-body interactions on the level of single particle properties. Generally speaking, the optical potential can be seen as merely another expression for the self-energy. However, its meaning has been narrowed to a purely imaginary quantity which depends only on the kinetic energy of the particle. There exist several formal relationships, especially between optical potential and energy, which have been approximatively derived and are valid in a more or less restricted energy range, like the parabolic approximation around the Fermi energy of Luttinger's Fermi liquid [1].

The proper access to that quantity, however, is offered by the self-energy which continuously lies in the focus of theoretical interest but only recently in the context of band structure calculations has been numerically quantified by refined approximations. [2, 3, 4] These are based on the GW approximation developed by Hedin. [5] Even within that approximation further simplifications are necessary specifying the type of dielectric function which is used in the screening of the Coulomb interaction yielding W in GW. Another line, followed in this paper, regards the self-energy as a functional of the ground state density in a local approximation, i.e. taken from the homogenous electron gas. Its energy and non-local k dependence can be retained.

Thus, it reflects the energetic shift and the damping of the quasiparticle as a non-groundstate property being derived for a local situation with given density. Early calculations for bulk metals basing on a similar reasoning denote that procedure as the "statistical approximation". [6, 7]

It is reasonable that e.g. the damping should be more efficient for higher electron density because of larger phase space for electron-hole or plasmon excitations. The properties of a one-dimensional model show that partly strong influences are to be expected by a lattice modulation of the optical potential. For example, a modulation in phase with the wave function amplifies the damping whereas anti-phase behavior compensates the effect of the homogenous part of the damping. [8]

In any case the general form of the self-energy will be a function of momentum transfer (non-locality), of frequency (dynamics), and of two reciprocal lattice vectors (local fields). The latter reflect the discrete translational symmetry of the lattice. This dependence is expected not to be far from diagonal behavior with weak variation of the diagonal elements with respect to momentum.

Another interesting point of view on the optical potential arises because of its intimate connection with the escape depth. Electron spectroscopies generally rely on the escape depth as that quantity which determines the surface sensitivity, or in an opposite sense, how far bulk properties can be detected in a specific range of a parameter set like electron propagation angle or energy. There is known an empirical dependence [9, 10, 11] on the latter quantitity which has been experimentally confirmed in the past within a large error bar but which only characterizes a rough not very lucidly stated correspondence. Some theoretical arguing on a homogenous electron gas basis is found. [12] A simple empirical relation for the variation of the escape depth with polar angle θ is given by $\cos\theta$. [13] The demand for a more clearly defined quantity than merely the mean free path together with a theoretical founding lies at hand because of growingly refined spectroscopies.

For example, photoemission as a spectroscopic tool for detecting valence properties gets information from bulk and surface as well. To decide which one of them is dominating depends on energy and angle. Actually, regarding full hemisphere angle acceptance accurate conclusions could be drawn with respect to the emitting region of the valence charge density if the detailed shape of final state wave function is known. [14] Opposite to the initial state being in the past the primary focus of band structure calculations the final state is not as commonly known. Directly accessible quantities such as the escape depth are preferred as a short cut over the still very demanding full one-step model calculations.

The quantification of the escape depth has to proceed via the calculation of the scattering state electron wave function and a suitable averaging. The solution of the Schrödinger equation depends on the choice of the optical potential which indirectly determines the decay length of the wave function from the surface into the crystal bulk. Here, we present the results of the calculation of the escape depth from the exact solution of the Schrödinger equation.

In the next section the types of approximations to be used are presented together with the procedures of numerical calculations. In the subsequent section the self-energy and the escape depth are discussed within the local density and the GW approximations.

1 CALCULATION

As long as the local density approximation is considered (used for GaAs) algebraic solvers are applied to the Schrödinger equation with asymptotic scattering boundary conditions. These conditions are transformed into a usual Dirichlet problem on a compact space via the so-called "Quantum Transmitting Boundary Method" (QTBM). [15, 16] The Laue representation is used discretizing in direct space with respect to the surface normal, i.e. the z-axis, and taking plane waves within the surface plane. In the case of the full calculation of $\mathbf{\Sigma}$ (used for $TiTe_2$) the scattering wave function is obtained via matching its value and derivative at the surface.

The local density approximation for the self-energy is obtained by parametrizing the results given by Lundqvist for the homogenous electron gas. [17] There the self-energy is shown only for energies fixed at the free particle energy of the actual momentum, i.e. usually near the maximum line in the $(\mathbf{k}, E)$ plane adequate for the case of well established quasiparticle properties. Thus, one degree of freedom is suppressed in this representation and two possibilities of an interpretation arise. In the dynamic picture which we adopt here only the energy is taken as an independent variable, the momentum being replaced via the free particle dispersion relation. This yields a purely local potential. In the nonlocal picture one would freely vary the momentum and replace the energy via its dispersion relation. Dynamical effects are suppressed by that procedure which was not used here. Its non-locality spoils the efficiency of the routines for solving the Schrödinger equation.

A formula was derived which fits the calculated self-energy [17] as a function of energy, E and electron density, $n(\mathbf{r})$. (Energies in eV)

$$\begin{aligned}
\mathrm{Im}(\mathbf{\Sigma}) &= a/(1.+\exp(-(E-\phi_t-\omega_p)/E_f))+d \qquad (1)\\
&\text{with}\\
E_f &= 13.6\frac{3.6831}{r_s^2}, \quad \text{Fermi energy;} \quad r_s = (\frac{3}{4\pi n(\mathbf{r})})^{1/3}\\
\omega_p &= 13.6\sqrt{12/r_s^3}+E_f, \quad \text{plasmon frequency;} \quad d = 0.12E_f\\
a &= \max((0.31r_s-0.24)E_f-d, 0)
\end{aligned}$$

To fit with the heuristic optical potential $\mathrm{Im}(\mathbf{\Sigma})$ has been additionally scaled by a factor of 0.5 when treating solely the valence part of the electronic charge. The vacuum threshold enters through ϕ_t. The charge of the valence states is calculated with the Extended Hückel Theory in the case of GaAs(110) [18]. It takes into account the surface relaxation.

The GW self-energy is obtained similar to a previous calculation [19] with a larger amount of its matrix elements and several values of the momentum within the

Brillouin zone. The computation of $\mathbf{\Sigma}$

$$\mathbf{\Sigma}_{G_1,G_2}(\mathbf{k},\omega) = \frac{ie^2}{(2\pi)^4\epsilon_0}\int d\mathbf{k}'\sum_{G'}\frac{1}{(\mathbf{k}-\mathbf{k}'+\mathbf{G_1}-\mathbf{G}')^2+\kappa_{TF}^2} \int d\omega' e^{i\omega'\delta}\epsilon^{-1}(\omega')G_{G',G'+G_2-G_1}(\mathbf{k}',\omega+\omega') \tag{2}$$

proceeds via an approximation of the dielectric function observing the exact energy dependence from an Extended Linear Augmented Plane Wave (ELAPW) [20] calculation but replacing the momentum dependence by a Thomas-Fermi relation with $\kappa_{TF} = 1.55$ Å^{-1} as deduced from the plasmon frequency of $\omega_p = 18$ eV for $TiTe_2$.

The theoretical escape depth could be defined and was investigated here in various ways. The characteristic structure did not depend sensitively on that choice for moderate escape angle. Thus, only one version is presented in the following. Namely, the z dependence of the density of the photoelectron wave function averaged over the two-dimensional unit cell is fitted to an exponential function with its exponent being defined as the reciprocal escape depth.

2 DISCUSSION

In Fig. 1 the self-energy is depicted in the GW approximation for $TiTe_2$. A matrix with respect to the reciprocal lattice vectors arises which is plotted vs. energy. The GW-$\mathbf{\Sigma}$ reveals a strong increase in its imaginary part above the plasmon frequency for all of the elements. The expected parabolic behavior is observed around the Fermi energy which may be approximatively extended also beyond the nearest neighborhood. The nondiagonal elements decrease with distance from the diagonal by orders of magnitude such that $\mathbf{\Sigma}_{G,G'}$ could be approximatively replaced by $\mathbf{\Sigma}_G\delta_{G,G'}$. As a function of G alone $\mathbf{\Sigma}_G$ is rather slowly varying with an asymptotic behaviour of $\propto 1/G^2$ for large G. Together with its finite value at $G = 0$ this could be approximated by an exponentially screened self-energy depending on $(z-z')$, only. In calculating the wave function a gradient expansion for the nonlocal contribution from $\mathbf{\Sigma}$ is not suitable in this energy regime in contrast to the bound states' regime. Instead, because the wave function is rapidly changing within the spread of the self-energy integral kernel, it is more adequate to approximate the shape of this kernel by a square well extending over the interval $(-r_s, +r_s)$ (atomic units). Thus, going beyond the local approximation it is preferable to consider as many neighbors as possible within that interval. For the purpose of comparison we considered in a separate calculation of the escape depth at most nearest neighbors because of computational burden using the very accurate algebraic solvers . However, in the presented figure the full $\mathbf{\Sigma}_{G,G'}(\omega)$ has been taken into account in solving the Schrödinger equation by direct matching at the solid-vacuum interface. The resulting escape depth is also plotted in Fig. 1 together with the real band structure. The main structure in the escape depth occurs at lower energies and coincides with the gaps of the band structure. At higher energies the structure is smoothed by the steeply increasing imaginary part of the self-energy. According to the usual heuristic values for the optical potential the smoothing was generally found too small in comparison with experiment. [21] The value obtained in this calculation for the optical potential significantly exceeds the heuristic one yielding an escape depth lowered by almost a factor of 3 at the maximum difference. Note that the heuristic formula saturates to a constant value near the plasmon frequency. The found behavior agrees much better with photoemission and results from total current spectroscopy (TCS). [21, 19]

For GaAs the local density form of the self-energy as derived from [17] under the aforementioned restrictions is applied. A general maximum at intermediate densities results from the vanishing damping for the density tending to zero and from the fact that for increasing density at fixed finite energy the reference Fermi energy with its zero damping increases reaching finally the fixed prescribed energy. This maximum will locally stress the damping by the valence electronic distribution around the atomic cores. Within the cores the high charge density excludes scattering by the exclusion principle and the lifetime becomes infinite.

The resulting escape depth is shown in Fig. 2 as a function of energy for two cases modelling the functional dependence on the density and for a third one with almost vanishing optical potential putting a, d both to 0.1 eV. Below 10 eV band structure effects originating from critical points dominate the shape. A similar and well pronounced energy dependence for all models is established which will influence the interpretation of electron spectra. A 50% increase of the damping on an interval of 2 eV reveals a dramatic change in the surface sensitivity. In tracking back for example the origin of a photoelectron advantage may be drawn from this behavior. Above about 15 eV differences appear with respect to the strength of the overall increase of the optical potential produced by the onset of plasmon losses. In the first model only the valence charge density is taken into account, in the second one the full core charge is regarded. Though the damping is vanishing within those very high density core regions the neighboring regions show an enhanced damping as seen in the following plot and the escape depth is depressed in the latter model because the wave function of the scattering state is mainly concentrated on the interstitial (anti-bonding) region. Small structures are observed also in the high energy range which are absent within the homogenous damping. Especially, the feature near 70 eV seems to be related to the Bragg scattering occurring at that energy. In agreement with the one-dimensional model [8] this structure might be associated with the scattering state's density distribution which is shifted in direct space from its position taken below such a gap in comparison with that taken above, thus experiencing different damping regions. These features are remarkable because at that energy usually they would have been damped out. The case of homogenously vanishing damping is shown to illustrate the structures to be expected if the optical potential were more reduced.

As a byproduct the total current spectrum (TCS) was obtained also for GaAs. By the shoulder at 15 eV in part (b) it confirms, see Fig. 2 (b) and (c), a previous suggestion [22] about a second experimental current minimum which has to be attributed to a second gap in the band structure, however, which was not found through a VLEED calculation (part (c)) with muffin-tin potentials in the cited paper. It is clearly a consequence of the pseudopotential used here. A technical detail might be worth mentioning. For the total current the reflected amplitude Φ^- has to be determined which appears in the relation

$$\psi(z) - e^{i\kappa z} = \Phi^- e^{-i\kappa z} \tag{3}$$

valid for all z within the vacuum region with constant potential. From the knowledge of the exact $\psi(z)$ it is numerically unstable to locally derive Φ^- from Eq. 3 because it would depend on the choice of z. It is more suitable to use

$$|\Phi^-|^2 = |\frac{\psi(z) - \psi(z-h)e^{i\kappa h}}{1 - e^{2i\kappa h}}|^2 \tag{4}$$

which shows to be roughly independent of h and z for large z where the image potential can be neglected. Several changes in the choice of parameter values have been tested with a rather weak effect on the escape depth showing that its energy dependent shape is dominantly affected only by the gaps in the single particle spectrum and by the increase of the scattering near the plasmon frequency.

However, a significant sensitivity occurs with changing the escape direction. The lower part of Fig. 3 shows the escape depth for energies within (part (c)) and at the upper edge (part (d)) of the gap appearing around 7 eV in the band structure for normal emission, see Fig. 2. Via the local approximation the charge density modulates the imaginary part of the self-energy as shown in the upper part Fig. 3. It is clearly seen how the high charge distribution within the cores (right picture) reduces the scattering to zero. A high charge density corresponds to a high "local Fermi energy" such that at the chosen energy the damping vanishes for these regions because the Pauli principles excludes any excitations. In any case, the strongest damping occurs in an intermediate region between the cores and the interstitial identified within the plot by the slightly darker edges surrounding the outer atomic spheres. The model displayed in Fig. 3(a) shows additional inner spherical parts of strong damping. This influences the energy dependence of the escape depth different from the homogenous damping yielding the wiggles as observed in Fig. 2. In the hemispherical plot of the escape depth one notices the small value for 7 eV and the high value for 10 eV in the center. This difference referring to the middle and the upper edge of the gap and being concentrated around the center proves that the escape depth probes the gaps also with respect to the direction. Thus, the strong features outside the center should be associated with directions of different transparencies either due to gaps in reciprocal space or due to paths through regions of high optical potential in direct space. It is not obvious what causes a specific structure. This is resolved only by considering the band structure in that direction.

In summarizing the self-energy has been calculated in two models, the GW and the local density approximation. The high energy damping turns out to be stronger than expected from the heuristic formulas. The escape depth has been obtained from solving the wave equation for the scattering states. It shows a modulation in energy and angle by the band structure which is strong below and still visible above the plasmon energy, especially in displaying the band gaps. Energetic structure which appears for higher energies is only observed with the inhomogenous optical potential, thus indicating agreement with the predicted modulation near Bragg resonances.

3 ACKNOWLEDGEMENTS

This work was supported by the Bundesministerium für Bildung und Wissenschaft under contract no. 05 SB8FKA7 and no. TSR-075-97. Grants of the Land Schleswig-Holstein are gratefully acknowledged.

References

[1] J.M. Luttinger, Phys. Rev. **121**, 942 (1960)

[2] M.S. Hybertsen, S.G. Louie, Phys. Rev. B **34**, 5390 (1986)

[3] M. Rohlfing, P. Krüger, J. Pollmann, Phys. Rev. B **48**, 17791 (1993)

[4] B. Wenzien, P. Käckel, F. Bechstedt, G. Cappellini, Phys. Rev. B **52**, 10897 (1995)

[5] L. Hedin, Phys. Rev. **139**, A796 (1965); L. Hedin, S. Lundquist, Solid State Physics **23**, 1 (1969)

[6] C.J. Tung, J.C. Ashley, R.H. Ritchie, Surf. Sci. **81**, 427 (1979)

[7] D.R. Penn, Phys. Rev. B **35**, 482 (1987)

[8] I. Bartoš, phys. stat. sol. (b) **122**, K159 (1984)

[9] C.J. Powell, Surface Sci. **44**, 29 (1974)

[10] P. Pianetta, J. Lindau, C.M. Garner, W.E. Spicer, Phys. Rev. B **18**, 2792 (1978)

[11] G. Ertl, J. Küppers, *Low Energy Electrons and Surface Chemistry*, VCH, Weinheim (1985)

[12] J.J. Quinn, Phys. Rev. **126**, 1453 (1962)

[13] C.S. Fadley, *Basic Concepts of X-ray Photoelectron Spectroscopy* in "Electron Spectroscopy: Theory, Techniques and Applications", C.R. Brundle and A.D. Baker, eds (Academic Press, London, 1978), **2**, p. 124

[14] C. Solterbeck, W. Schattke, J.-W. Zahlmann-Nowitzki, K.-U. Gawlik, L. Kipp, M. Skibowski, C.S. Fadley, M.A. Van Hove, Phys. Rev. Lett. **79**, 4681 (1997)

[15] C.S. Lent, D.J. Kirkner, J. Appl. Phys. **67**, 6353 (1990)

[16] S. Lorenz, C. Solterbeck, W. Schattke, J. Burmeister, W. Hackbusch, Phys. Rev. B **55**, R13432 (1997)

[17] B.I. Lundqvist, phys. stat. sol. **32**, 273 (1969)

[18] F. Starrost, S. Bornholdt, C. Solterbeck, W. Schattke, Phys. Rev. B **53**, 12549 (1996)

[19] W. Schattke, Prog. Surf. Sci. **54**, 211 (1997)

[20] E.E. Krasovskii, Phys. Rev. B **56**, 12866 (1997)

[21] A. Bödicker, PHD thesis, Kiel (1996)

[22] J.-V.Peetz, W.Schattke, H.Carstensen, R.Manzke, M.Skibowski, Phys. Rev. B **46**, 10127 (1992)

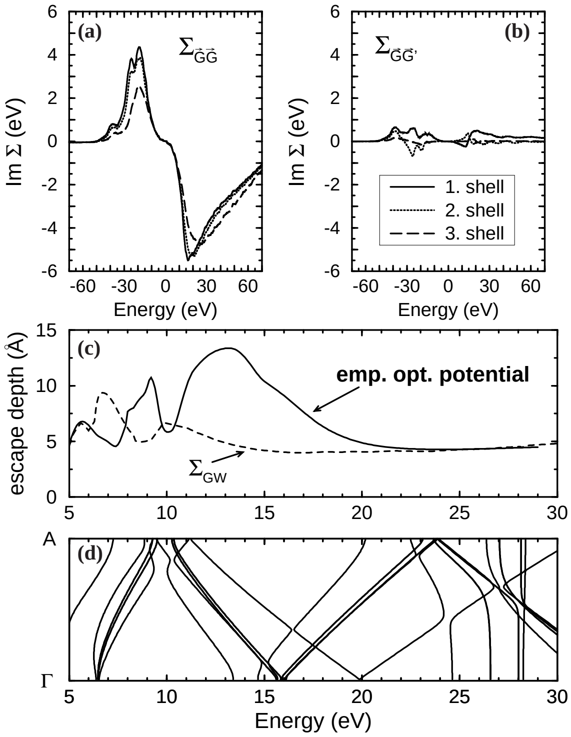

Figure 1: Upper part: Self-energy matrix of $TiTe_2(0001)$ for the first three shells of the reciprocal lattice, $\mathbf{G}_i, i = 1,2,3$; $\mathbf{G}_1 = (0,0,0), \mathbf{G}_2 = (0,0,2\pi/c), \mathbf{G}_3 = (1/3, 1/\sqrt{3}, 0)2\pi/a$; diagonal elements part (a), the nondiagonal elements (part (b))carry the index pairs (1,2),(2,3),(3,1); lower part: Escape depth of normal emission for the heuristic modelling (solid) and the full incorporation of $\mathbf{\Sigma}_{G,G'}(\omega)$ (dashed) together with the real band structure (below)

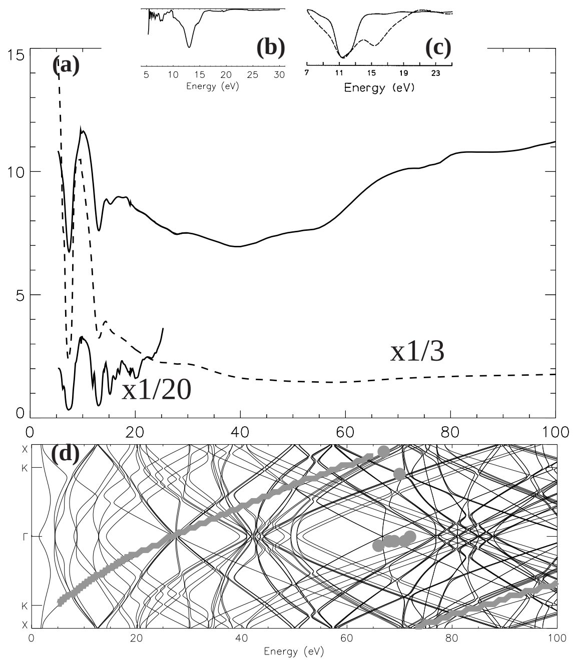

Figure 2: Part (a): Escape depth of normal emission with the bandstructure (part (d)) for GaAs(110) for three models of the density functional (see text), comprising the valence charge only (solid), including also the atomic cores (dashed) or with almost vanishing optical potential (lower solid); the main emitting complex band is shown (shaded); insert: Theoretical (solid) and experimental (dashed) TCS-curves (current-voltage characteristics) for normal incidence, part (b) this calculation, part (c) from reference [22]

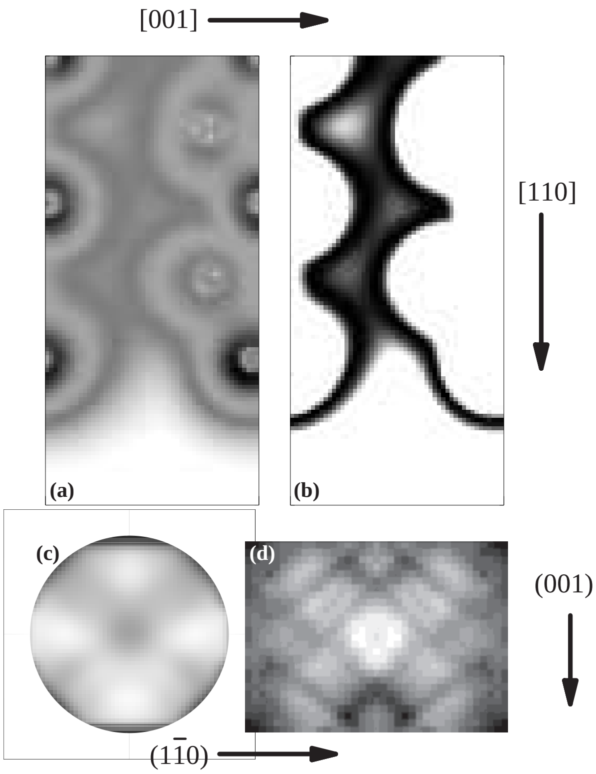

Figure 3: Upper part: Imaginary part of the self-energy at 10 eV over the (1$\bar{1}$0) surface in real space for the model without (part (a)) and with (part (b)) inclusion of the full core charge; bright regions correspond to small | Im$\boldsymbol{\Sigma}$ |; lower part: Escape depth over the (110) surface of momentum space for kinetic energy 7 eV over the full hemisphere (part (c)) and 10 eV over the 1. Brillouin zone (part (d)) above valence band maximum; bright regions correspond to high escape depth